

# FEA Based Design of Outer Rotor BLDC Motor for Battery Electric Vehicle

Rupam<sup>1</sup>, Sanjay Marwaha<sup>2</sup>, Anupma Marwaha<sup>3</sup>

<sup>1</sup>Research Scholar, Department of Electrical and Instrumentation, SLIET, Sangrur, India, rupamb92@gmail.com

<sup>2</sup>Professor, Department of Electrical and Instrumentation, SLIET, Sangrur, India, marwaha\_sanjay@yahoo.co.in

<sup>3</sup>Professor, Department of Electronics and Communication, SLIET, Sangrur, India, marwaha\_anupma@yahoo.co.in

\*Correspondence: rupamb92@gmail.com

**ABSTRACT-** Due to enormous advantages, BLDC motors have been identified for the design in various applications. With its good power density, this motor is being used by the automobile industry. The paper aims to design the motor for the battery electric vehicle. The major challenge of the BLDC motor is to reduce torque ripples which appear because of high cogging torque. Torque ripple results in acoustic noise and vibrations in the battery electric vehicle which badly affects the performance of the vehicle. The cogging torque and efficiency are characterized by a parametric technique with varying pole embrace factor and magnetic thickness. The selection of optimum values of rotor pole embrace factor and magnetic thickness has a significant role in the reduction of cogging torque. The Ansys Maxwell tool helps in the optimum designing of the motor by mitigating the torque ripples and thus increasing the average torque. The proposed model has 5.7% better efficiency in comparison to the base model and has a small number of torque ripples.

**Keywords:** Cogging torque, BLDC, Ansys Maxwell, Torque ripple, Magnet thickness.

## ARTICLE INFORMATION

**Author(s):** Rupam, Sanjay Marwaha, Anupma Marwaha;

**Received:** 13/08/2022; **Accepted:** 29/10/2022; **Published:** 20/12/2022 ;

**E- ISSN:** 2347-470X;

**Paper Id:** IJEER220745;

**Citation:** 10.37391/IJEER.100459

**Webpage-link:**

[www.ijeer.forexjournal.co.in/archive/volume-10/ijeer-100459.html](http://www.ijeer.forexjournal.co.in/archive/volume-10/ijeer-100459.html)



**Publisher's Note:** FOREX Publication stays neutral with regard to jurisdictional claims in Published maps and institutional affiliations.

## 1. INTRODUCTION

The permanent magnet Brushless DC motor (PMBLDC) is well recognized in predetermined categories of motors used for design and in everyday applications [1]. Robotic nurses equipped with BLDC motors have been deployed to provide essential vitamin-infused foods and medications to persons impacted by the COVID'19 epidemic. The BLDC motor is also used by drones that are used to monitor social distance and spray sanitizer [2-3]. Therefore, this motor has recently experienced an inescapable rise in the market, and researchers can still demonstrate their contribution to improving the rise in the market recently, and researchers can still demonstrate their contribution to the improvement of these PMBLDC motor's performance. These motors have a well-acknowledged role in the automotive drive industry applications [4]. Nowadays, BLDC motors are often used and popular due to their remarkable benefits in the automotive drive industry. The excellent efficiency and emission-free design of electric vehicles allowed them to reach a wide audience before the effects of COVID'19. Many automotive sectors are giving priority to BLDC motors in testing their electrified vehicle designs. To assure improved characteristics, the cogging

torque is a relatively difficult problem in BLDC motors that demands an urgent solution [5-7].

The techniques for reducing cogging torque and enhancing torque quality can generally be divided into two categories. The first method presents modification in motor design to reduce the pulsating torque component. The second one relies on control strategies to change the stator excitation waveform to produce smooth torque [8]. Numerous adjustments to geometrical structures have been documented in the literature to ensure that cogging torque is minimized. In one of the studies, the design of the motor was proposed based on the best selection of pole and slot combinations for applications like light electric vehicles [9]. The design of the BLDC motor was proposed either by varying slot/pole combination, altering magnet thickness, and embracing to enhance the performance of the motor in-wheel BEV [10-12]. The author proposed the design of a surface-mounted axial flux BLDC motor to give the best possible combination of design variables acquired by employing the optimization technique genetic algorithm (GA), and the motor design depends on these optimized design factors [13]. The authors designed the claw pole shape type sub-fractional horsepower BLDC motor for reducing the cogging torque [14]. The effect of the motor performance was analyzed with stator notch modification in the design to reduce torque ripple [15]. The author proposed optimal design by showing the effect of the pole embrace factor for BEV applications [16]. The author designed a surface-mounted type motor by selecting the appropriate combination of pole arc coefficient, pole, and slot with help of the FEM tool [17]. The computational numerical finite element method (FEM) is used to determine the electromagnetic analysis among the machines [18]. Without any significant knowledge of applied mathematics, this method can be used to determine

electromagnetic field distribution and integral parameters in the design of the rotating machine. An extensive amount of research has been done on the design of motors using FEM [19-23]. The geometrical optimization results in the reduction of the torque ripple and demagnetization of parameters. For the specific application, the outer rotor type was selected instead of the inner rotor. The outer rotor motor is used as a direct drive for medium and low-speed vehicles. This enhanced the power and torque density of the motor which positively affects the performance of an electric vehicle.

This paper analyses the performance of the outer rotor BLDC motor having a 4/12-pole/slot with the help of the FEM tool. An analytical method establishes a link between the output torque of the motor and its aligned rotor position. The main objective of the presented work is to show the effect of change of rotor pole embrace factor value and magnetic thickness on the performance of BLDC motor. The FEM-based tool has been used to analyze the magnetic field density and plot the mesh. The proposed model yields reduced cogging torque and increase the efficiency at the optimal value of pole embrace factor and magnetic thickness with parametric analysis.

## 2. METHODOLOGY AND PARAMETER MATCHING OF MOTOR

### 2.1 Parameter matching of BEV

The kinematic dynamic equations are considered for calculating the parameters of the BEV with the BLDC motor. With the use of initially presumptive parameters, the driving resistive forces and ratings of the vehicle have been determined using the EV characteristics [24]. The battery electric vehicle ratings are tabulated in *table 1*.

**Table 1. Specifications of initial parameters for BEV**

Parameter	Value
Weight (m)	100 Kg
Specific acceleration (g)	9.81 m/s <sup>2</sup>
Coefficient Rolling resistance ( $\mu_r$ )	0.004
Vehicle Dimensions radius (r)	0.33 m
Density of air ( $\delta$ )	1.23 Kg/m <sup>3</sup>
Drag coefficient ( $C_d$ )	0.45

### 2.2 Mathematical modeling of BLDC motor

The underlying principles for the working of a BLDC motor are the same as for a brushed DC motor; i.e., internal shaft position feedback. In the case of a brushed DC motor, feedback is implemented using a mechanical commutator and brushes. With a BLDC motor, it is achieved using multiple feedback sensors. The most commonly used sensors are hall sensors and optical encoders. Voltage and current will continue to have phase variations to increase the motor's electromagnetic torque [8, 17]. In BLDC motors, cogging torque is position-dependent which results from the magnetic field interaction around the permanent magnets on the rotor and stator teeth with steel lamination. The permanent magnets

are positioned in relation to the stator teeth to determine the least amount of reluctance. The cogging torque reduces the motor's average torque and causes the motor to experience unpleasant torque ripple. When the motor is energized with constant current, cogging torque causes a variance in torque production termed torque ripples. These ripples produce fluctuations and jerkiness at slower speeds. To reduce noise and vibration it is necessary to eliminate cogging torque. This may cause damage to the machine and reduce the position target accuracy. The cogging torque can be represented in *equation (1)* where  $T_c$  is the cogging torque, flux air gap  $\phi_g$ , air gap reluctance is  $R$  and  $\theta$  is the rotational angle.

$$T_c = 0.5(\phi_g^2)(dR/d\theta) \quad (1)$$

The pole embrace factor is calculated as the fraction of the rotor pole arc to rotor pole pitch which is affected by the electrical rotor degree also. The number of rotations, the strength of the magnetic field, and the position and speed of the rotor all have an impact on the back-EMF readings. Back-EMF values for various phases are illustrated in *equation 2* is the back-EMF constant ( $\lambda$ ).

$$\begin{aligned} e_a &= \omega \lambda (\theta) \\ e_b &= \omega \lambda (\theta - 120) \\ e_b &= \omega \lambda (\theta + 120) \end{aligned} \quad (2)$$

The electromagnetic torque is represented in *equation (3)*. The torque at any instant of the rotor is the sum of the average torque and torque ripple for the motor is represented as in *Equation (4) and (5)* where  $(\theta'_1 - \theta_1)$  represents the complete electrical cycle, and  $T(\theta)$  is the torque at any rotor angle of the motor.

$$T_e = P_1 / \omega \quad (3)$$

$$T_{avg} = (1 / (\theta'_1 - \theta_1)) \int T(\theta) \quad (4)$$

$$T_{ripple} = (T_{max} - T_{min}) / T_{avg} \quad (5)$$

## 3. DESIGN AND ANALYSIS OF MOTOR

### 3.1 Design aspects and Parameter solutions

Using ANSYS Maxwell software, the outer rotor BLDC model has been created for a 500 W rating. The dimensional specification of the designed model is listed in *table 2*.

**Table 2. Initial specifications of BLDC motor**

Parameter	Values
Stator Outer Dia ( $D_{so}$ )	108
Stator Inner Dia ( $D_{si}$ )	62
Steel Type	Steel_1010
Rotor Outer Dia ( $D_{ro}$ )	140
Axial Length (L)	55
Magnet Type	NdFe35

One of the design parameters selected to observe the performance of the BLDC model is the pole embrace factor of the rotor. An overview of 4 poles, and 12 slots outer rotor BLDC motor is shown in *figure 1*. The outcome of the

proposed model is compared with [25] the inner rotor model of the BLDC motor.

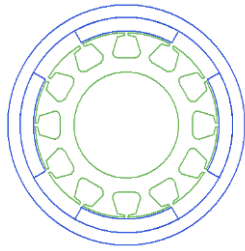


**Figure 1:** Overview of outer rotor BLDC motor

The pole embrace factor is selected as a variable under the parametric method and gradually changed from initial step 0.5 to final step 0.85 with a step size of 0.05, to decrease the cogging torque value. The optimum value must be determined from total values, including intermediate values under sensitivity analysis. *figure 2* illustrates a graphical representation of cogging torque versus embrace factor as a result of parametric solutions.

The graphical representation of the variation of cogging torque and rotor degree is presented in *figure 3*. It is observed that when the value of the embrace factor is extremely close to 0.65 the lowest cogging torque component value found is 0.237 Newton-meter found. The cogging torque is highest at the initial point 0.5 of the embrace factor which is 0.544 Nm. The graphical representation of efficiency with the variation of pole embrace is shown in *figure 4*. At this point, the highest efficiency 92.4% of the motor is also observed.

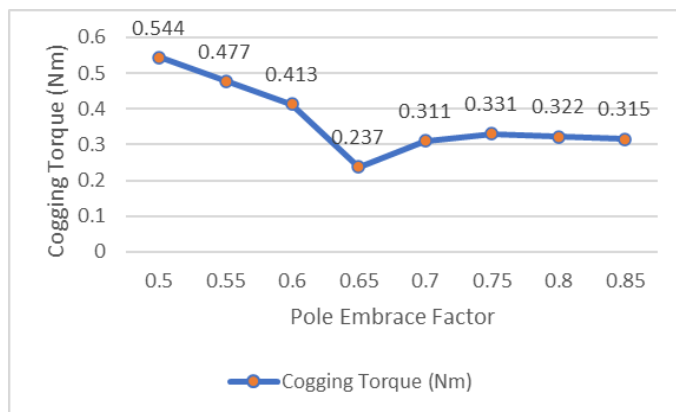


**Figure 2:** Cogging Torque versus Pole Embrace

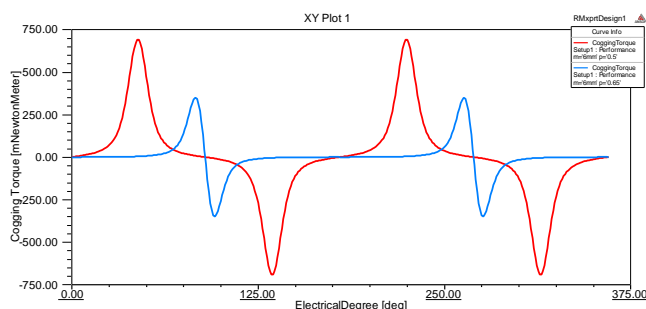


**Figure 3:** Comparison of Cogging Torque at initial and optimum value

Another effective variable magnet thickness is varied from 6 mm to 12 mm with a step size of 1 mm under parametric analysis to achieve high efficiency. The representation of efficiency with magnet thickness is shown in *figure 5*. It is observed at value 8mm the efficiency of the motor is 92.4 % which matched with the previous variable. The highest efficiency and lowest cogging torque are determined at the optimal value of 0.65 pole embrace and 8 mm magnet thickness. The graphical representation of efficiency with the variation of rotor speed is shown in *figure 6*. The speed of the rotor is varied up to 3000 rpm and the efficiency of the motor gets highest when the speed is near about 2700 rpm.

The optimum value of the variable selected for the outer rotor BLDC motor is 8 mm magnet thickness and 0.65 pole embrace factor having efficiency achieved is 92.4% which is 5.4% highest than the inner rotor BLDC motor [25].

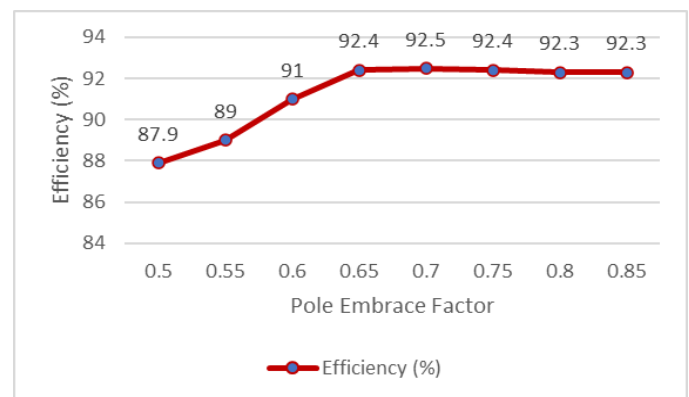


**Figure 4:** Efficiency with pole embrace factor

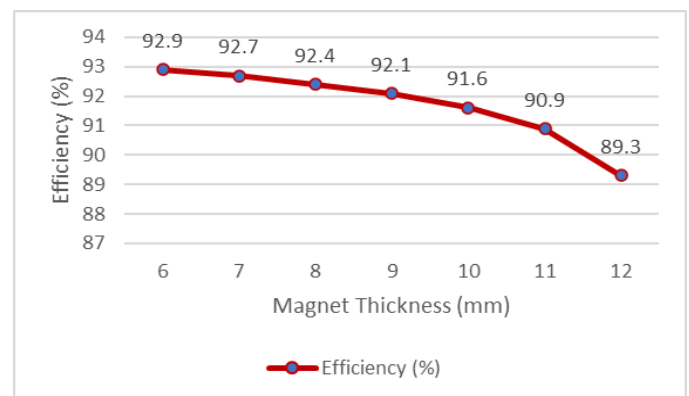


**Figure 5:** Efficiency versus magnet thickness

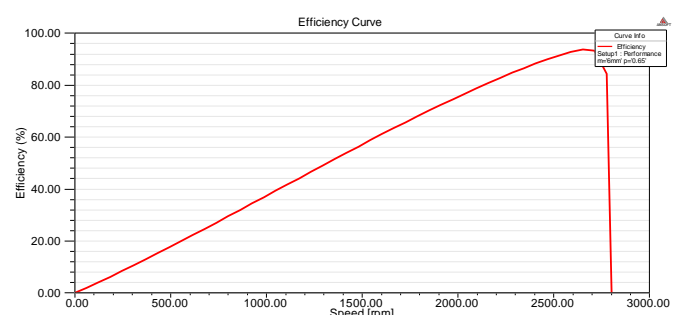


**Figure 6:** Efficiency with rotor speed

### 3.2 Finite element analysis of the proposed motor

For the evaluation of electromagnetic issues, the model is built using a computational electromagnetic tool ANSYS Maxwell. The model is based on the periodic boundary condition of the motor with inner magnetic field distribution. To expedite the computation speed of the motor, one-fourth part of the model is considered for the simulation. *Figure 7* depicts a mesh plot of the outer rotor BLDC motor at its optimum value of design variable i.e., magnet thickness of 8 mm and pole embrace factor of 0.65. The total elements determined are 2050 for the mesh plots of the model.

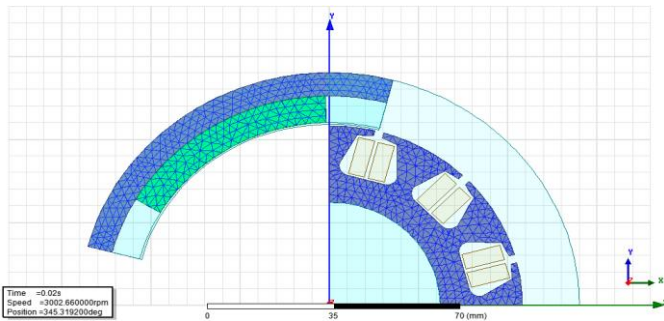


**Figure 7:** Mesh plot of the model

The magnetic field density distribution profile for a specific time and for a specific position of rotor angle is shown in *figure 8*. It investigates the distribution of the magnetic field at any time and position. The motor is running continuously at the rated speed and it can be observed that the stator has a maximum magnetic flux density of 1.8T and is distributed simultaneously across the vector boundary of the model. The model has better magnetic strength than the outer rotor model of BLDC for a specific application.

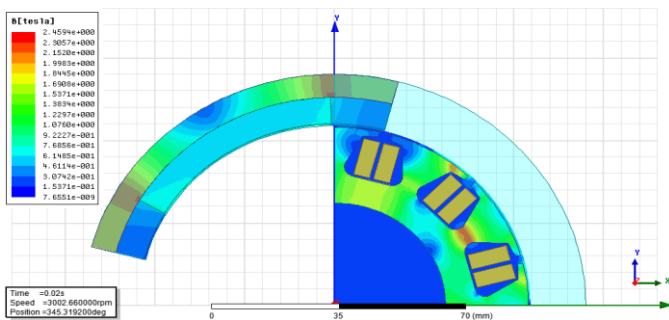


**Figure 8:** Magnet field distribution of the model

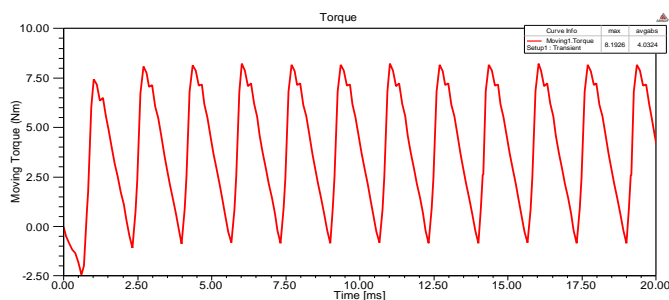


**Figure 9:** Variation of electromagnetic torque versus time

The FEM-based transient field analysis of the model has been done for moving torque response at any instant of time. The variation of electromagnetic torque versus the time is shown in *figure 9*. The torque ripple of the model has a value of 2.17 with maximum torque of 8.1 Nm and average torque of 4.03 Nm.

The efficiency of the optimum model has increased by 5.7% and achieved the required rated parameters with less cogging torque in comparison to the base model [25]. However, the significant reduction in torque ripples will increase the life span of the motor with minimum regular maintenance requirements. The results of the proposed model have satisfied the parameters of particular reference BEV.

## 4. CONCLUSION

The proposed design of the motor is suitable for the battery electric vehicle application. This paper aims to illustrate the effect of rotor pole embrace parameters and magnetic thickness on motor performance. It's evident the electrical cycle and rotor pole embrace factor have been connected analytically. It is found that cogging torque is decreased by adjusting the pole embrace factor using parametric analysis. The optimal value of magnet thickness observed for the determination of higher efficiency of the proposed model. Based on the parametric analysis the optimum value of pole embrace factor and magnet thickness is determined using a FEM tool. The computed value of cogging torque decreases from 0.544 Nm to 0.237 Nm at optimum point of pole embrace factor 0.65. It is seen that proposed model has efficiency 92.4% which is 5.4% highest value than the inner rotor model of motor. The model has better magnetic field strength and at optimum point the value of torque ripple is 2.17. This reduced the vibrations of the motor which enhance the overall performance of the battery of the vehicle. For this model, further additional core loss analysis can look at a variety of other reliable geometric parameters to identify other performance parameters.

The present work emphasizes mainly the computation of electromagnetic parameters related to an electric vehicle. For the holistic analysis of the vehicle, in the future, the Multiphysics analysis pertaining to temperature and vibrations may be attempted. Moreover, finite element refinement strategies such as h-type, hp-type may be considered for comparative analysis. Further, an attempt may be made to examine the hierarchical finite element technique in the domain under consideration.

## 5. ACKNOWLEDGMENTS

Sant Longowal Institute of Engineering and Technology, Punjab, India for providing access to licensed Ansys Maxwell software and supporting the overall work.

## REFERENCES

- [1] Lee, S. K., Kang, G. H., Hur, J., & Kim, B. W. (2012). Stator and Rotor Shape Designs of Interior Permanent Magnet Type Brushless DC Motor



- for Reducing Torque Fluctuation. IEEE Transactions on Magnetics, 48(11), 4662-4665.
- [2] Jain, G., Chauhan, D., Meen, Y., & Bunker, N. S. (2022). Application of Quad rotor drone to Combat COVID-19: A review. International Journal of Research in Engineering and Science, 10(2), 13-20.
  - [3] Harfina, D. M., Zaini, Z., & Wulung, W. J. (2021). Disinfectant spraying system with quadcopter type unmanned aerial vehicle (UAV) technology as an effort to break the chain of the COVID-19 virus. Journal of Robotics and Control (JRC), 2(6), 502-507.
  - [4] Palomino, A., Parvania, M., & Zane, R. (2021). Impact of covid-19 on mobility and electric vehicle charging load. In 2021 IEEE Power & Energy Society General Meeting (PESGM) (pp. 01-05). IEEE.
  - [5] Dalal, A., & Kumar, P. (2018). Design, prototyping, and testing of a dual-rotor motor for electric vehicle application. IEEE Transactions on Industrial Electronics, 65(9), 7185-7192.
  - [6] Alias, A. E., & Josh, F. T. (2022). Design Analysis of SSD Optimized Speed Controller for BLDC Motor. International Journal of Electrical and Electronics Research (IJEER), 10(3), 529-535.
  - [7] Shahapure, S. B., Kulkarni, V. A., & Shinde, S. M. (2022). A Technology Review of Energy Storage Systems, Battery Charging Methods and Market Analysis of EV Based on Electric Drives. International Journal of Electrical and Electronics Research (IJEER), 10(1), 23-35.
  - [8] Hanselman, D. C. (2003). Brushless Permanent-Magnet Motor Design. The Writers' Collective.
  - [9] Liu, C., Zhu, J., Wang, Y., Lei, G., Guo, Y., & Liu, X. (2015). Design and analysis of an outer rotor flux switching permanent magnet machine for electric vehicle. In 2015 IEEE International Magnetics Conference (INTERMAG) (pp. 1-1). IEEE.
  - [10] Ocak, C., Tarimer, I., Dalcı, A., & Uygün, D. (2016). Investigation effects of narrowing rotor pole embrace to efficiency and cogging torque at PM BLDC motor. TEM Journal, 5(1), 25-31.
  - [11] Cabuk, A. S., Sağlam, Ş., & Üstün, Ö. (2017). Impact of various slot-pole combinations on an in-wheel BLDC motor performance. IU-Journal of Electrical & Electronics Engineering, 17(2), 3369-3375.
  - [12] Ocak, C. E. M. İ. L., Dalcı, A., Çelik, E. M. R. E., & Uygün, D. (2017). FEA-Based design improvement of small scale BLDCMs considering magnet thickness and pole embrace. Int'l Journal of Computing, Communications & Instrumentation Engg, 4(2), 31-35.
  - [13] Patel, A. N., & Suthar, B. N. (2018). Design optimization of axial flux surface mounted permanent magnet brushless dc motor for electrical vehicle based on genetic algorithm. International Journal of Engineering, 31(7), 1050-1056.
  - [14] Leitner, S., Gruebler, H., & Muetze, A. (2019). Cogging torque minimization and performance of the sub-fractional HP BLDC claw-pole motor. IEEE Transactions on Industry Applications, 55(5), 4653-4664.
  - [15] Perianayagam, C. A., Krishnakumar, V., & Dhanushvarma, R. (2020). Stator Notching Design of Permanent Magnet Brushless DC Motor to Mitigate the Cogging Torque. In 2020 IEEE International Conference on Power Electronics, Drives and Energy Systems (PEDES) (pp. 1-6). IEEE.
  - [16] Guo, L., & Wang, H. (2021). Research on Stator Slot and Rotor Pole Combination and Pole Arc Coefficient in a Surface-Mounted Permanent Magnet Machine by the Finite Element Method. World Electric Vehicle Journal, 12(1), 26.
  - [17] Rupam, Marwaha, S. (2021). Mitigation of Cogging Torque for the Optimal Design of BLDC Motor. In 2021 IEEE 2nd International Conference on Electrical Power and Energy Systems (ICEPES) (pp. 1-5). IEEE.
  - [18] Chan, C. C., & Chau, K. T. (1991). Design of electrical machines by the finite element method using distributed computing. Computers in industry, 17(4), 367-374.
  - [19] Kumar, A., Marwaha, S., Singh, A., & Marwaha, A. (2009). Performance investigation of a permanent magnet generator. Simulation Modelling Practice and Theory, 17(10), 1548-1554.
  - [20] Kumar, A., Marwaha, S., Singh, A., & Marwaha, A. (2010). Comparative leakage field analysis of electromagnetic devices using finite element and fuzzy methods. Expert Systems with Applications, 37(5), 3827-3834.
  - [21] Kumar, A., Marwaha, S., Marwaha, A., & Marwaha, A. (2009). Comparative Mechanical Dynamic Analysis of Permanent Magnet Generator Using Finite Element and Fuzzy Methods. The Open Automation and Control Systems Journal, 2(1).
  - [22] Sharma, S. K., & Manna, M. S. (2022). Finite Element Electromagnetic Based Design of Universal Motor for Agro Application. International Journal of Electrical and Electronics Research (IJEER), 10(3):590-596.
  - [23] Ehsani, M., Gao, Y., Longo, S., & Ebrahimi, K. M. (2018). Modern electric, hybrid electric, and fuel cell vehicles. CRC press.
  - [24] Mithunraj, M. K., Warriar, G. S., Pathivil, P., Kanagalakshmi, S., & Archana, R. (2019). Design and performance analysis of brushless DC motor using ANSYS Maxwell. In 2019 2nd International Conference on Intelligent Computing, Instrumentation and Control Technologies (ICICICT) (Vol. 1, pp. 1049-1053). IEEE.



© 2022 by Rupam, Sanjay Marwaha, Anupma Marwaha. Submitted for possible open access publication under the terms and conditions of the Creative Commons Attribution (CC BY) license (<http://creativecommons.org/licenses/by/4.0/>).